AD-A062 550 CRANFIELD INST OF TECH (ENGLAND) SCHOOL OF MECHANICA--ETC F/G 21/5
UNSTEADY EFFECTS OF CIRCUMFERENTIAL PRESSURE DISTORTED INLET FL--ETC(U)
NOV 78 R E PEACOCK AFOSR-77-3305

UNCLASSIFIED AFOSR-TR-78-1629 NL

| OF |
AD
A062550

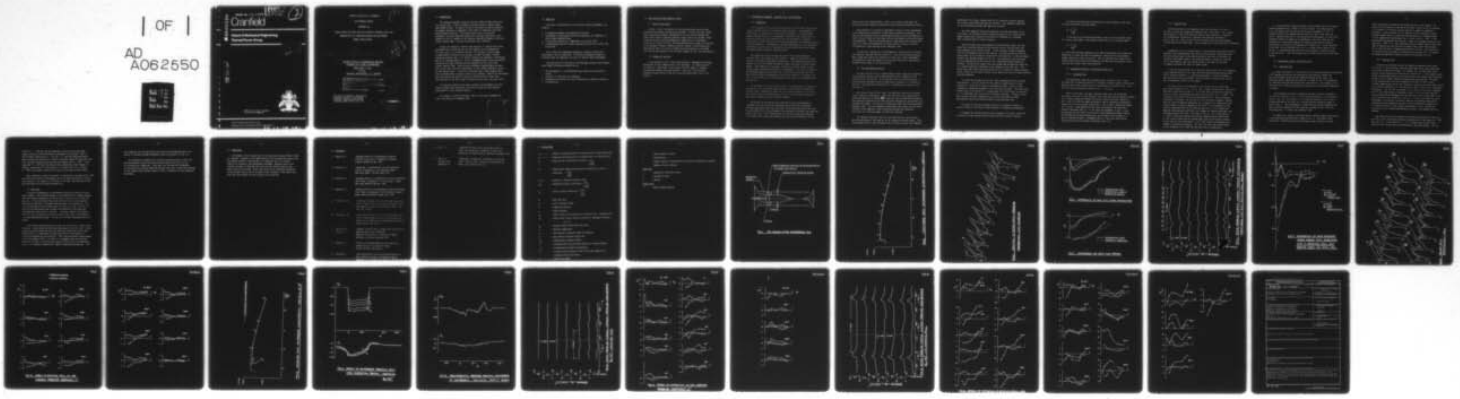

AFOSR-TR- 78-1629

LEVEL II

3

Cranfield

School of Mechanical Engineering

Thermal Power Group

Cranfield Bedford MK43 0AL England
Telephone 0234 - 750111 (Bedford 750111) Telex 825072

CRANFIELD INSTITUTE OF TECHNOLOGY

THIRD PROGRESS REPORT

PREPARED FOR

UNITED STATES AIR FORCE OFFICE OF SCIENTIFIC RESEARCH (AFSC) USA

EUROPEAN OFFICE OF AEROSPACE RESEARCH AND DEVELOPMENT

LONDON, GREAT BRITAIN

UNSTEADY EFFECTS OF CIRCUMFERENTIAL PRESSURE DISTORTED INLET FLOWS IN COMPRESSORS.

GRANT AFOSR-77-3305

(061392)

PRINCIPAL INVESTIGATOR: R. E. PEACOCK

The School of Mechanical Engineering
Cranfield Institute of Technology
Cranfield, Bedford, Great Britain
Telephone (0234) 750111, Ext. 523

November 1978

39 p.

1.0 INTRODUCTION

The research programme covered by the grant AFOSR-77-3305 arises from the proposal (Ref. 1) which followed a previous period of research under grant AFOSR-74-2708. The overall thrust of this work has been to establish the dynamic behaviour of compressor rotor blades in compressor inlet flow maldistributed conditions. This may be seen as part of an overall programme to evaluate compressor behaviour in unsteady conditions, a programme conceived in response to the observed reduced performance of aero-gas turbine engines under a variety of disturbed inlet conditions.

Because the compressor internal flow behaviour is rapidly time variant experiments must include the use of high response rate instrumentation. The rotor, which in a distorted flow sees, for instance, a quasi-steady circumferential distortion as an unsteady, variable incidence, variable stagnation pressure flow, is of special interest and challenge in the measurement of its unsteady behaviour. Hot-wire anemometry may be used successfully outside of the rotor plane but the data measured can only infer rotor channel internal flows. While hot-wire anemometry unquestionably has many uses in this area, the direct measurement of rotor dynamic behaviour carries its own special value. It was for such reasons that a high response rotor-borne instrumentation system was conceived at Cranfield. Much of its development took place during the period of the grant AFOSR-74-2708 and rotor data were presented in the final report covering the work under that grant (Ref.2)

The research covered by this grant includes the development of a high speed peripheral data acquisition and analysis system and more detailed measurements of rotor unsteady features.

This report is the third progress report in this work programme and covers the period up to November 1978.

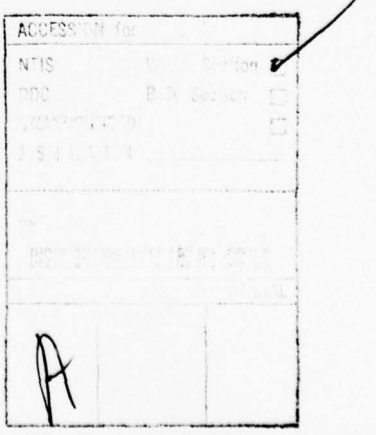

2.0 OBJECTIVE

The overall long-term aim of the Cranfield research programme is to produce:-

1. an improved parameter for quantifying distortion
2. improvements in performance prediction techniques for compressors in quasi-steady distorted flows
3. a prediction technique for compressors in pulsating flows
4. a design method that will reduce compressor sensitivity to inlet flow distortions.

This involves an integrated programme of research in which five experimental rigs are being used. In parallel, mathematical models of distorted flows and compressor reactions to them are under development.

The detailed aim of that part of the programme covered by the research grant AFOSR-77-3305 may be quantified as:

1. the development of a custom-designed data acquisition and analysis system
2. evaluation of rotating stall phenomena
3. evaluation of distortion on rotor transients and compressor behaviour
4. flow modelling

3.0 DATA ACQUISITION AND ANALYSIS SYSTEM

3.1 General Description

In Refs. 3 and 4, the details of the custom designed and built data acquisition and analysis system were presented. In brief, two rotor blades each carrying high response instrumentation at the blade mid-height with eight static pressure tappings generates signals which pass through a multiplexor board with associated temperature compensation to a peripheral system via a 24 way slip ring. Following amplification signals are digitised in an analogue to digital converter and pass through a 16K microprocessor which may be used in a variety of modes from data-logging on a cartridge unit for off-line analysis on an ICL 1903T computer to real time data-analysis.

3.2 Progress of the Unit

It was reported in ref. 4 that late delivery of components had delayed manufacture but that commissioning trials had begun. An intensive series of checks has taken place in the course of which a number of software and hardware problems have been resolved. This work is now virtually complete and application of the unit in gaining experimental data is now imminent.

4.0 EXPERIMENTAL PROGRAMME - ROTATING STALL INVESTIGATIONS

4.1 Background

The existence of large-scale non-uniformities in the inlet flow of axial compressors has recently received widespread attention. The mathematical difficulties in handling other than linearised models of such flows have however limited theoretical developments: furthermore, the complexities of data acquisition and presentation and even the development of suitable parameters by which to describe these unsteady phenomena have severely hampered the experimentalist. Nevertheless, continued improvement to axial compressor performance, particularly in surge-margin and operating range, must include an improved understanding of unsteady effects.

For compressors operating near the surge line, the development of rotating stall cells appear to be a common or maybe universal (Ref. 5.6), precursor to complete breakdown of performance. This phenomenon consists of regions or cells of retarded flow moving around the annulus relative to the blades. Axial symmetry is destroyed, resulting in stalled blades in parts of the annulus and unstalled blades in the remainder. The stall cell moves in the direction against that of the rotor, relative to the blades, but since the relative speed of propagation is usually less than the rotor speed, the cell is seen to move in the same direction as the rotor in an absolute frame of reference.

The presence of the stall cells results in a deterioration of compressor performance since the maximum pressure ratio is not achieved in regions of retarded flow. Furthermore, since this self-induced distortion is periodic, the forced frequencies generated may coincide with the natural harmonics of the blading, tending to cause structural damage.

The effects of non-uniform inlet conditions and the development of rotating stall are clearly not unrelated; one results from an external influence upstream of the stage, the other can be generated within the blade row, but both result in non-axisymmetric and therefore unsteady flow conditions within rotor rows. The distortions may be from one to many blade passages in circumferential extent and therefore have associated frequencies of the

order of the rotor rotating speed. These are of course, much lower than the blade passage frequencies encountered when considering blade wake effects.

Described here is a series of experiments in which a fully instrumented axial compressor was tested over a wide range of operating conditions. Not only was the compressor overall performance obtained, but the distribution of static pressure along the rotor blade surfaces was measured with high response instrumentation. Data were obtained both for undistorted and distorted inlet flows, the latter being generated by uniform porosity screens of various circumferential extent mounted at the compressor inlet.

Of particular interest was the development of rotating stall cells when the compressor operated near the surge-line. The on-rotor pressure measurements showed very clearly the formation of these cells, whose development, circumferential extent and speed of rotation were found to be significantly affected by the nature of the upstream flow.

4.2 The Experimental Facility

The test rig (fig.1) was a lightly-loaded, single stage axial compressor, having constant annulus cross-section measuring 25.4 cm diameter at the hub and 50.8 cm. at the tip. All blades were built up from C4 sections. A variable-speed, 5hp motor drove the compressor at speeds up to a maximum of 1500 rpm. The massflow was controlled by a throttle-valve situated at the tailpipe exit.

The rig was fitted with the usual instrumentation required to evaluate overall compressor performance. Inner and outer wall static tappings were positioned ahead of and behind every blade row, and the downstream stagnation pressures were measured by four rakes disposed orthogonally, each having nine shrouded pitot heads. All pressure readings were taken from inclined multiple manometer banks. Hot wire anemometer measurements were taken with the probe situated in the compressor inlet, providing both mean and turbulence velocities for a selected number of operating conditions.

The compressor pressure ratio was calculated from the total pressure measured downstream of the stage by the 36 stagnation pressure probes. Using the averaged value of static pressure from the inner and outer wall tappings

downstream of the stage, together with the 36 stagnation pressure readings, the velocity distribution was obtained radially. Area weighted integration of this distribution yielded the compressor massflow.

The rotor speed was measured by mounting a 60 tooth gear wheel on the drive shaft. An inductive pick-up sensed the passage of each tooth and the number counted over a period of one second was displayed on a frequency meter (yielding speed in rev/min directly).

Two rotor blades were instrumented at blade mid-height (bmh), one with eight static pressure tappings on the pressure surface, and the other with eight tappings on the suction surface. A high-frequency response transducer (70 kHZ) was mounted at bmh for each tapping. The pressure was fed from the blade surface to the transducer volume within the blade via a 0.038 cm diameter transfer tube (maximum length of 0.152 cm). The transducers had a miniature silicon diaphragm (0.318 cm) on which a full Wheatstone bridge network was diffused. The electrical output wires were routed down through the blade root to a remotely-controlled switching circuit mounted on the rotor disc. The signals were then taken from the rotating rig via a precision slipring assembly (noise $<5\mu V/ma$) to an external switch control device and finally to amplification / recording equipment.

The system was designed so that any eight transducers could be recorded simultaneously. This was wired for four channels (combinations) of eight transducers. Selection of channel A connected the eight pressure surface transducers to eight galvanometers in an ultraviolet recorder. The other three channels were: B) 8 suction; C) 4 leading edge (LE) suction and 4 LE pressure; D) 4 trailing edge (TE) suction and 4 TE pressure tappings. Channels C and D were included to permit time-matching of suction and pressure surface measurements (taken from different blades) during unsteady flow.

The entire pick-up and recording system had a frequency response in excess of 4000 Hz, sufficiently high to handle all frequencies encountered.

A yawmeter was located one-half chord upstream of the rotor, permitting calculation of the upstream static pressure and inlet relative velocity.

The blade surface pressure distribution data were evaluated in the usual pressure coefficient (C_p) form, where:-

$$C_p = \frac{p - p_1}{\frac{1}{2}\rho W_1^2}$$

In the case of the unsteady experiments, where only time averaged values of p_1 and V_1 were known, a new pressure coefficient C* was utilised, where:-

$$C^* = \frac{p - p_\theta}{\frac{1}{2}\rho W_1^2}$$

p_θ is the static pressure measured at the same blade tapping at the same flow conditions in steady flow and the denominator represents the time-averaged dynamic pressure as seen by the rotor. Thus C* represents the change in the blade surface static pressure distribution resulting from the presence of the rotating stall and/or inlet flow distortion.

4.3 Experimental Results in Undistorted Inlet Flow

4.3.1. Unstalled Flow

The experimental compressor performance map is shown in fig. 2. Data are shown for ten operating points at a constant rotational speed of 1250 rev/min. Measured rotor blade surface pressure distributions are plotted in fig. 3 for the nine unstalled operating conditions (a - i) of fig 2.

While at the higher and lower incidences these data show unexpected excursions, they are in good agreement with other data near the design incidence. Fig. 4 shows a comparison between the present results and those reported in Ref. 7 and 8 for similar blades operating at similar incidences and Reynolds' numbers for rotor and cascade respectively. Fig. 5 shows a comparison between the present experimental data and those calculated by the analytical method of Martensen (Ref. 9). In all cases the agreement is good. It may be observed that the ripple in the convex surface measured by Rhoden (Ref.8) and followed by the data reported here, was ascribed to the presence of a laminar separation bubble, a phenomenon which, in any case, could not be predicted by the inviscid model of Martensen (Ref. (9).

4.3.2 Rotating Stall

Further reduction of the compressor mass flow from point i of fig. 2 to point j led to the inception of rotating stall in the rotor. Fig. 6 shows the variation of rotor blade pressure surface static pressure as a function of circumferential location at a constant flow condition indicated by point j (fig. 2). Data are given for seven chordal locations, with tapping 1 being nearest the leading edge. Rotor movement was in the direction of increasing θ.

Examination of fig. 6 reveals that at a given tapping, the pressure pattern repeated itself approximately every 540^{o} of absolute rotor rotation and thus the stall pattern moved in the same direction as the rotor at one-third its rotational speed when viewed in the absoluted frame of reference. Relative to the rotor however, the stall pattern moved in the opposite direction at roughly two-thirds the rotor rotational speed.

It may also be seen from fig. 6 that the rotating stall cell first appeared at the rearmost portion of the rotor blade and moved upstream requiring about 20^{o} of relative rotation (i.e. three blade passages) to reach the leading edge and become fully established. The cell occupies roughly 20 per cent of the circumferential extent to the annulus.

The data of fig. 6 are replotted in the form of pressure coefficient and chordal dimension in fig. 7 and 8. Fig. 7 shows a comparison of the results obtained in the unstalled flow ($i = 11.9^{o}$) with those for flow with rotating stall at a point circumferentially remote from the stall cell ($\theta = 660^{o}$). The incidence at the latter condition was approximately 14^{o}. Given the modest difference in incidence, the two results are in excellent agreement, showing that the flow had adequate opportunity to re-establish its steady state flow pattern between successive passages of the stall (a key assumption in the parallel compressor model of the rotating stall flow.) Fig. 8 shows the measured rotor pressure coefficient for a number of azimuthal positions (the reference position for $\theta$and θ' are shown in fig. 6). It is clear that at $\theta = 180^{o}$ a significant pressure distribution change had been experienced by the suction surface and the leading edge region of the pressure surface. By the time the rotor had moved to $\theta = 225^{o}$ both surfaces experienced gross changes in pressure distribution. Not until the rotor had rotated nearly a full revolution (to $\theta = 540^{o}$) was the flow fully re-established.

To illustrate more clearly the effect of the rotaing stall cell on blade element performance fig. 9 shows a plot of C*v chord. The reference state for p_θ and hence C* was the pressure distribution obtained at $\theta = 45^o$, a condition sufficiently removed from the stall cell that 'clear flow' prevailed. Absolute values of C* are not particularly meaningful in view of the averaging required in computing the denominator, but shifts from the zero reference are a qualitative measure of change in blade surface pressure distribution as a result of the pressure of rotating stall. As was observed by Day (Ref. 10) the rotating stall cell is a highly active region of flow; and this is supported by these data; The rapid changes of surface pressure in the region of $\theta \approx 405^o$ are evidence that reversed flow existed in the blade passage.

4.4 Experimental Results in Distorted Flow

4.4.1 Unstalled Flow

To assess the effects of inlet distortion on the blade pressure distributions a 90^o squarewave distortion was generated by positioning a uniform low porosity wire-mesh screen one-half diameter upstream of the stage. The resulting overall compressor characteristic is shown in fig. 10 superimposed for comparison upon the undistorted flow characteristic. The movement of the stability line, yielding a surge-margin reduction for an operational compressor, is evident.

The associated variation of stagnation and static pressure upstream of the stage is indicated in fig. 11 for the operating points q-v on the characteristic (fig. 10). A discussion of the seemingly anomolous rise in static pressure upstream of the rotor as it emerged from the distortion region is given in Ref. 7. The corresponding circumferentially varying stagnation and static pressures downstream of the stage are presented in fig. 12 for an operating point, v, close to the stability limit.

An example of a typical rotor blade concave surface pressure distribution at the same operating condition is shown if fig. 13. The blade clearly experienced a significant pressure disturbance every revolution, but the

effect was generally limited to the forward portion of the passage. The effect of the distortion screen may be seen more clearly in fig. 14 in which C* is plotted as a function of blade chord for a number of tangential locations. In this instance C_θ* is a measure of the difference in static pressure between that at a given and that prevailing at a reference value of θ for comparatively undisturbed flow - in this case at $\theta = 150^o$. If the undistorted flow pressure distribution is taken to correspond roughly to that shown for $\theta = -90^o$, it is clear that major pressure changes began to take place some 30^o before the rotor entered the shadow of the screen and persisted for at least 60^o after it emerged from behind the screen. This observation is consistent with the spread in upstream static pressure (fig. 11) and the corresponding downstream stagnation pressure distribution (fig.12).

4.4.2 Rotating Stall

Closure of the throttle to move the compressor operating point from v to w on fig. 10 led into what, from instrument observation, may be described as a classic rotating stall mode. For example, fig. 15 shows rotor blade concave surface pressure distributions as a function of θ. While superficially similar to those data found in the rotating stall case without inlet distortion screens (fig. 6) several important differences may be observed. The period of the rotating stall cell cycle lengthened from 540^o to 720^o of rotor rotation, meaning that the cell was rotating at one-half the rotor speed relative to a stationary observer (c.f. one-third rotor speed in the case of undistorted inlet flow). Thus the cell was moving at $U/2$ relative to the rotor, compared with $2U/3$ for flow without a distortion screen. It is also clear that the pressure perturbation propagated from the leading to the trailing edge of the blade, unlike the undistorted flow case (fig 6) in which the reverse was true. Furthermore, on alternate revolutions, when the instrumented blade passed through the screen shadow but the stall cell was diametrically opposite in the compressor annulus, only a minor perturbation in static pressure was experienced at the forward three measuring station. The remainder were unaffected.

The rotor blade surface pressure distributions were plotted in the form of C^*v^x/c in fig. 16 where the reference condition for C* was taken at $\theta = 225^o$ (see fig. 15). In the region $0^o \leq \theta < 75^o$, following the transit of the stall cell the flow was being re-established in the blade passage. For the

range $75^{o} < \theta < 150^{o}$ the flow was apparently stabilized, the apparently unusual pressure distribution being a consequence of selecting $\theta = 225^{o}$ as the reference condition for C*. For $150^{o} < \theta < 330^{o}$ the blade experienced modest pressure fluctuations as a result of passing through the distorted inlet flow, but major pressure excursions did not commence until $\theta = 630^{o}$. In the range $630^{o} < \theta < 780^{o}$ the rotor blade clearly experienced rapid changes in loading, characteristic of the transit of a rotating stall cell. Finally ($\theta > 810^{o}$) the flow was restored to the state which prevailed 720^{o} earlier.

Other distortion screens of different circumferential coverage (15^{o} to 120^{o}) and varying porosity were investigated, but in no other instance was rotating stall observed. For example, a 15^{o} screen of the same (low) porosity as that described above did not produce rotating stall.

4.5 Discussion

It would be inappropriate to draw general conclusions from the limited data presented. The existence however of two different stall régimes suggests that two different mechanisms of rotating stall initiation on the rotor are possible. In the undistorted flow case, the rotor blade surface pressure distributions indicate a disturbance moving forward in the blade row. This is not inconsistent with the observations of others (e.g. Ref. 10) who, on the basis of observations made upstream and downstream of the blade row, concluded that reverse flow is possible. It further suggests the rotating stall cell has its origins in the stator and that the rotor is responding to a rotating downstream blockage. To check this, further experiments would be needed.

In the case of the distorted inlet flow, the stall cell is clearly rotor-initiated. The perturbation resulting from passage of the stall cell is much greater than that caused solely by the distortion screen and in fact, once rotating stall is established, the unstalled portion of the annulus is virtually unaffected by the distortion. This latter observation lends support to the stall model of Ref. 11 in which it is suggested that the unstalled portion of the flow is operating well below the stall line on the operating curve; it is therefore comparatively immune to upstream perturbations. This

flow, combined with the small mass flow rate passing through the stall cell, results in the mass-averaged performance given by the point w in fig. 10.

The inception of rotating stall and the flow pattern within a stall cell and the mechanism controlling the flow pattern within the stall cell are not currently well understood. These data, with the detailed information on flow within the rotating blade row may have some value in improving knowledge in this complex flow situation, which is still a limitation in axial compressor performance.

5.0 CONCLUSIONS

Two elements of the research work to be covered by the grant AFOSR-77-3305 are reported. Progress of the commissioning of the high speed data acquisition and analysis system is recorded and it is noted that this is virtually ready to be included in the experimental programme. Meanwhile data on the internal structure of rotating stall cells and the identification of two types of cell are presented. While these data are not immediately applicable to the designer they do add to the body of data available on the subject and they offer new insights into the rotating stall mechanism.

6.0 REFERENCES

1. Peacock R.E. 'Unsteady effects of circumferential pressure distorted inlet flows in compressors' Research Proposal 959:REP:132 Dec. 1976

2. Peacock R. E. 'Square-wave circumferential pressure distortion effects in compressors' Final Research Report USAF Grant AFOSR - 74-7208 March 1977

3. Peacock R. E. 'Unsteady effects of circumferential pressure distorted inlet flows in compressors' First Progress Report USAF Grant AFOSR-72-3305 Nov. 1976

4. Peacock R. E. 'Unsteady effects of circumferential pressure distorted inlet flows in compressors' Second Progress Research Report USAF Grant AFOSR-77-3305. April 1977.

5. Greitzer E. M. 'Surge and rotating stall in axial flow compressors, Part 1: Theoretical compression system model' Trans. ASME Journal of Engineering for Power, April 1976 Vol. 98, 190-198.

6. Greitzer E. M. 'Surge and rotating stall in axial flow compressors, Part II: Experimental results and comparison with theory' Trans. ASME Journal of Engineering for Power. April 1976 Vol 98, 199-211.

7. Peacock R.E. Overli, J. 'Dynamic internal flows in compressors with pressure maldistributed inlet conditions' AGARD-CP-177 46th P.E.P. Conference of AGARD Marterey, California September 1975

8. Rhoden H. G. 'Effects of Reynolds number on the flow of air through cascades of compressor blades' A.R.C. R & M No. 2919 (1952)

9. Martensen E. 'The calculation of the pressure distribution of thick aerofoils by means of Fredholm integral equations of the second kind' N.A.S.A. TTF-702 July 1971.

10. Day. I. J. 'Detailed flow measurement during deep stall in axial flow compressors' AGARD-CP-177 46th P.E.P. Conference of AGARD Marterey, California September 1975

11. Day I. J.
Greitzer E.M.
Cumpsty N. A. 'Prediction of Compressor performance in rotating stall' Trans. A.S.M.E. Journal of Engineering for Power. Jan. 1978 Vol 100, 1-12

7.0 NOMENCLATURE

$a, b \ldots j$ = compressor operating points on characteristic in undistorted flow

$q, r \ldots v$ = compressor operating points on characteristic in distorted flow

C_p = blade surface coefficient of pressure = $\dfrac{p-p_1}{\frac{1}{2}\rho_1 W_1^2}$

C^* = dimensionless blade surface pressure change due to stall or distortion = $\dfrac{p-p_\theta}{\frac{1}{2}\rho W_1^2}$

C.P.R. = compressor stagnation pressure ratio

$C_{\Delta T}$ = stagnation pressure coefficient = $\dfrac{P-P_1}{\frac{1}{2}\rho_o V_o^2}$

C_s = static pressure coefficient = $\dfrac{p-p_1}{\frac{1}{2}\rho V_o^2}$

M = Mass flow rate

N = rotor rotational speed

P = Stagnation pressure

p = static pressure

p_θ = blade surface static pressure in distorted flow rotating stall

Δp = blade surface static pressure relative to atmospheric pressure

$= p_\infty - p$

R_b = Reynolds'Number based upon blade chord

T = Absolute temperature

V = gas velocity in absolute frame of reference

W = gas velocity relative to the rotor

x/c = dimensionless chordal distance

θ = circumferential position with respect to a fixed reference

θ_D = circumferential extent of distortion

θ' = circumferential position of stall cell with respect to a reference fixed to the rotor

U = rotor blade speed

i = flow incidence to blade

ρ = fluid density

τ = angular extent of rotating stall cell period, expressed in absolute degrees of rotor rotation

Subscripts

o = upstream of distortion screen

1 = upstream of rotor

∞ = ambient

Superscripts

$\bar{}$ = mass averaged quantity

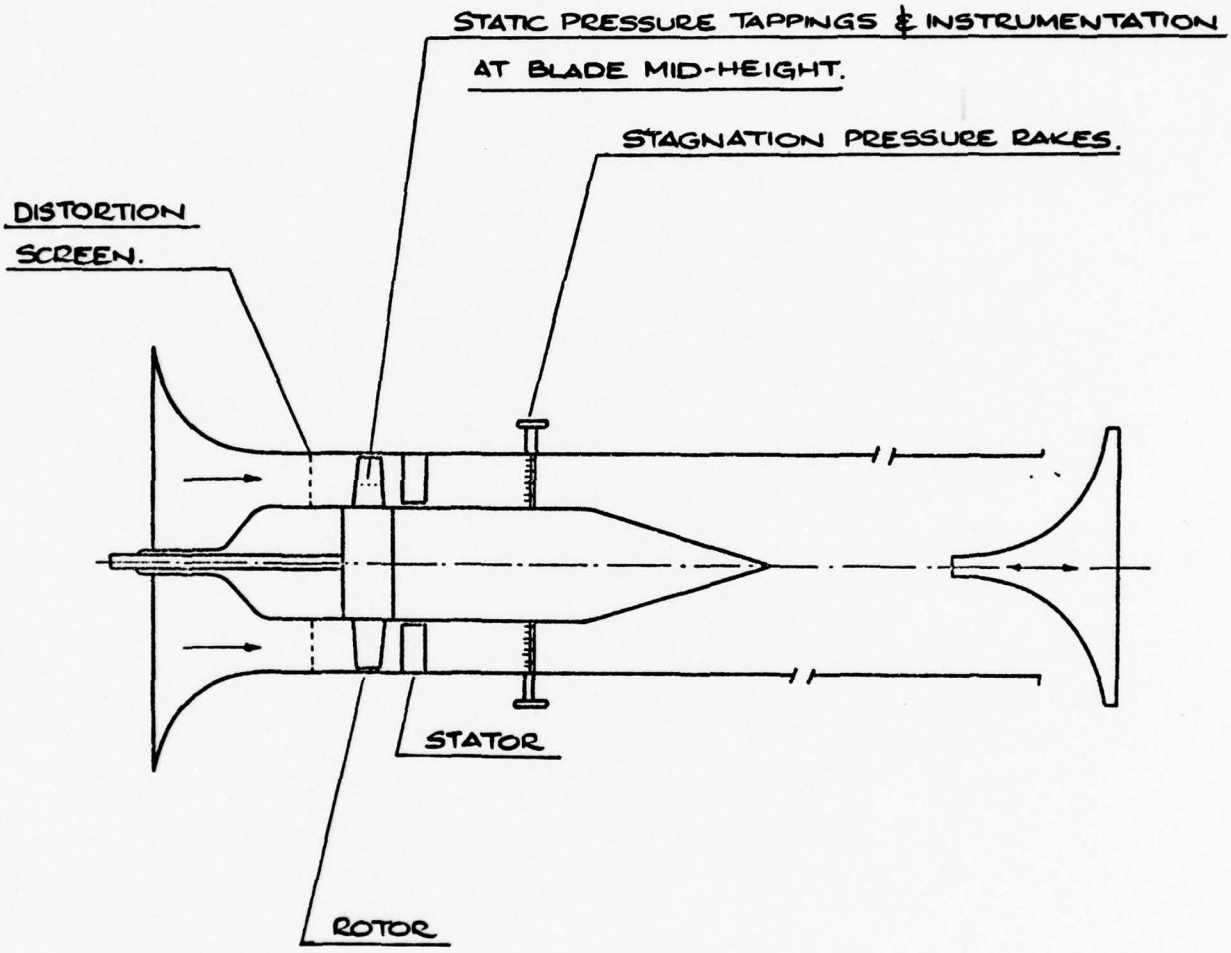

FIG. 1. THE SINGLE STAGE COMPRESSOR RIG

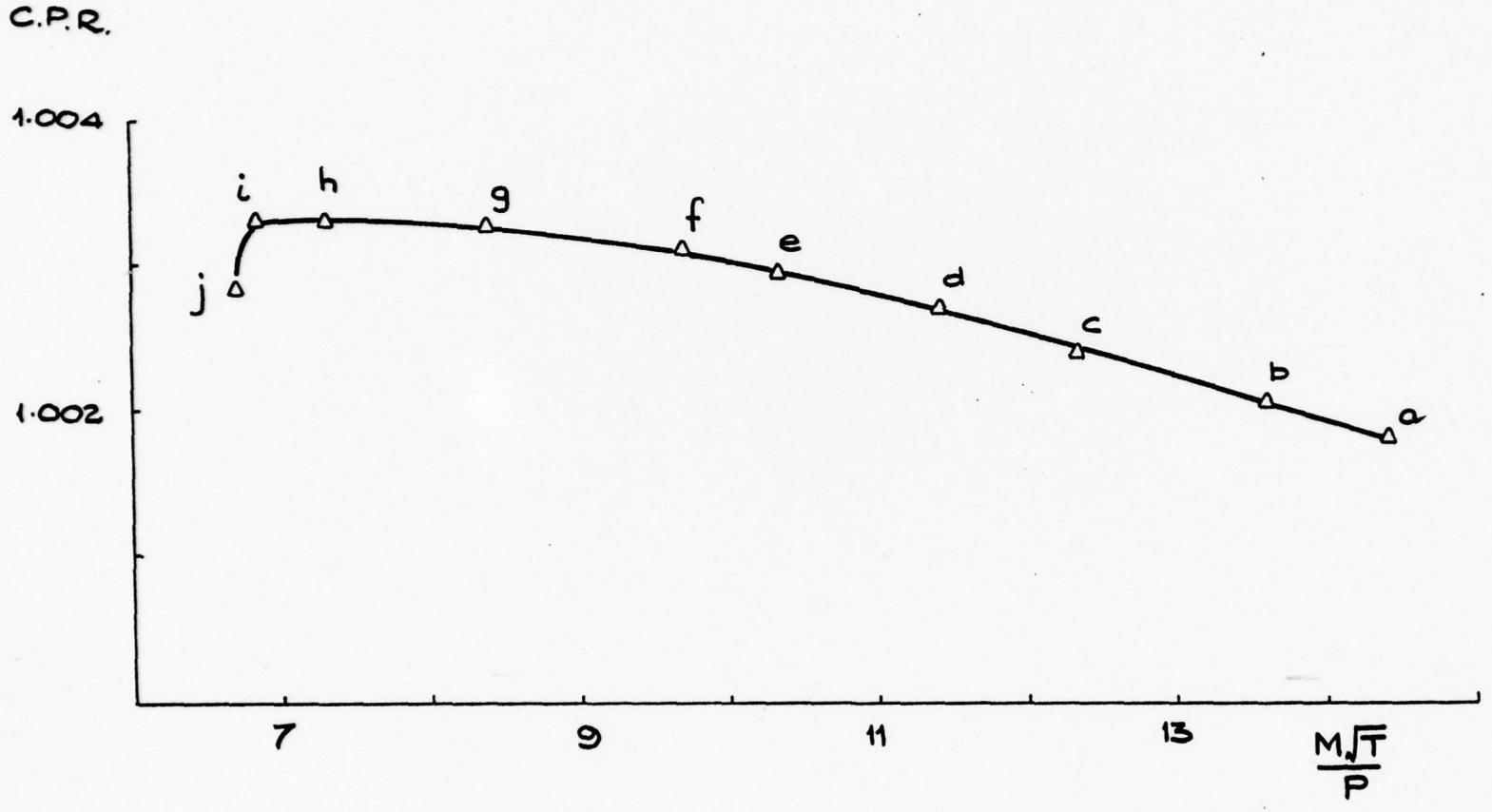

FIG. 2. UNDISTURBED COMP COMPRESSOR CHARACTERISTIC - 1250 rev/min

FIG. 2

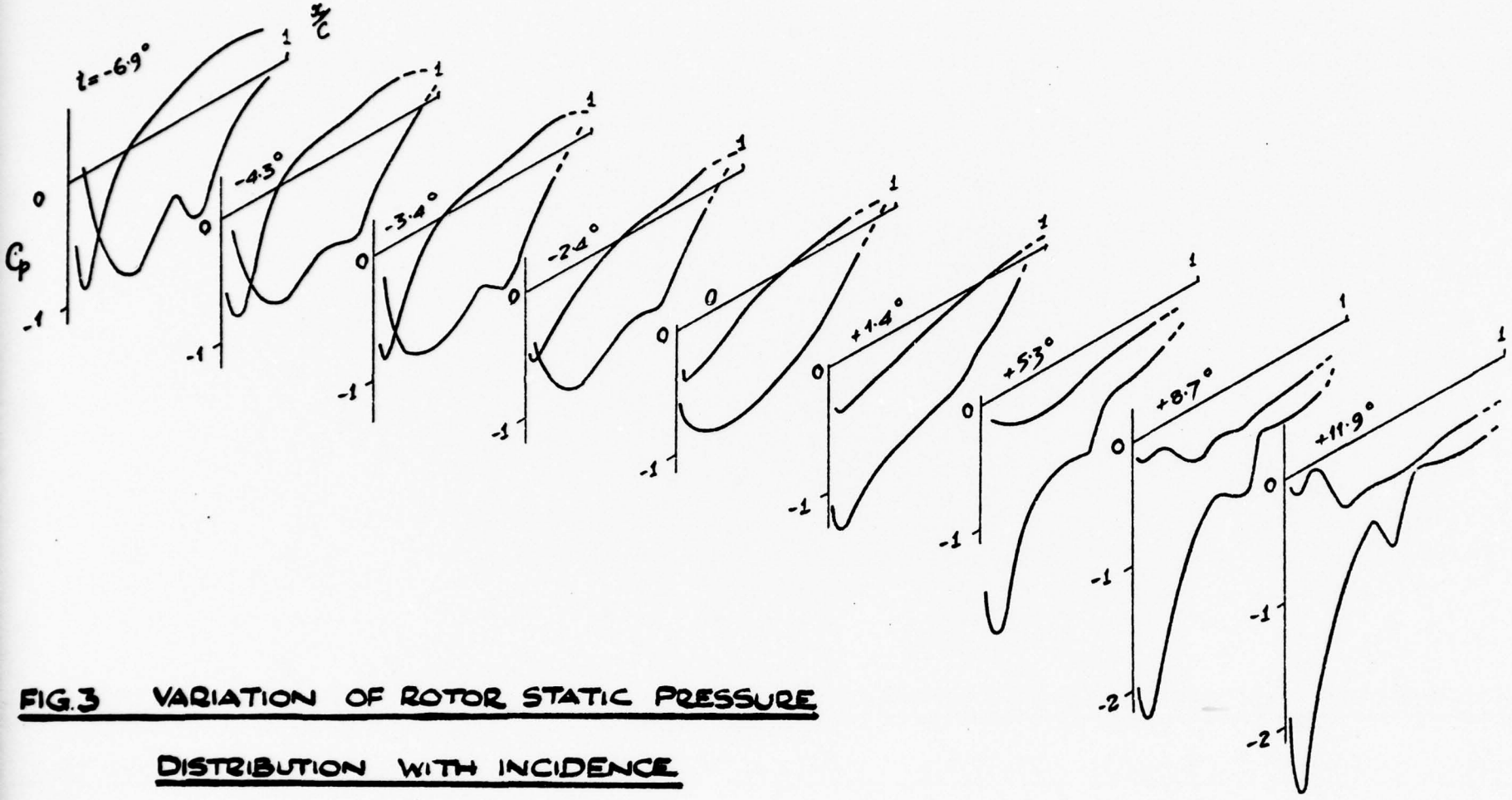

FIG.3 VARIATION OF ROTOR STATIC PRESSURE DISTRIBUTION WITH INCIDENCE

FIG.3

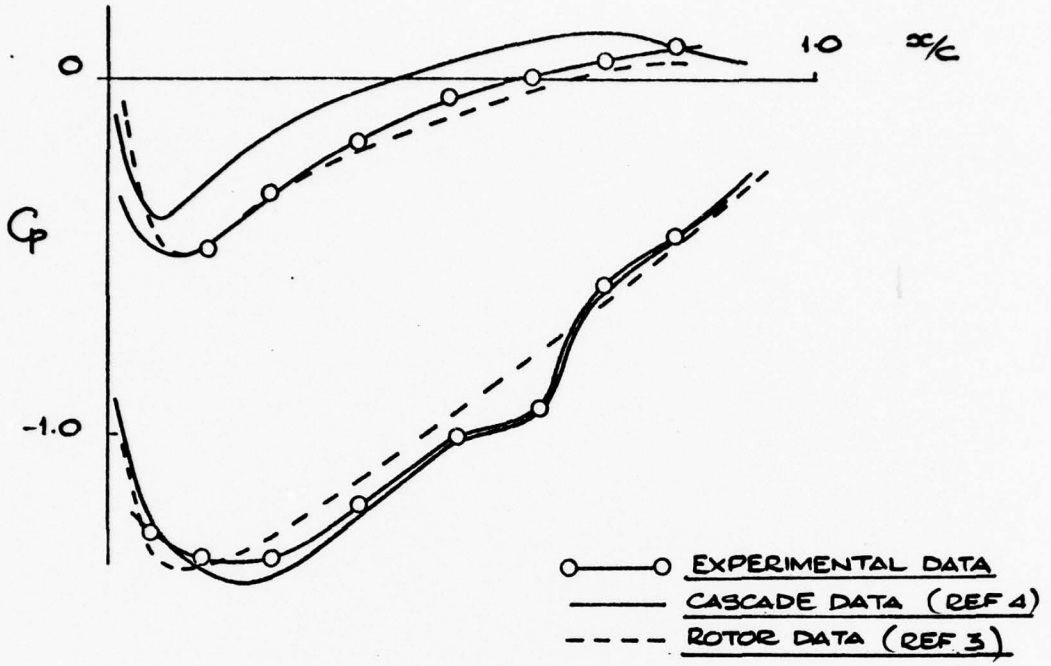

FIG 4. COMPARISON OF DATA WITH OTHER EXPERIMENTS

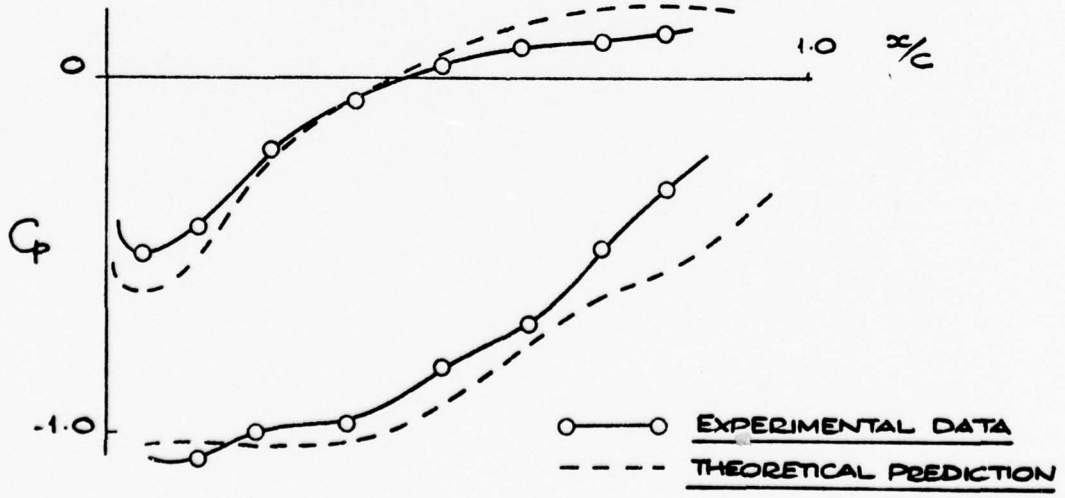

FIG 5 . COMPARISON OF DATA WITH THEORY

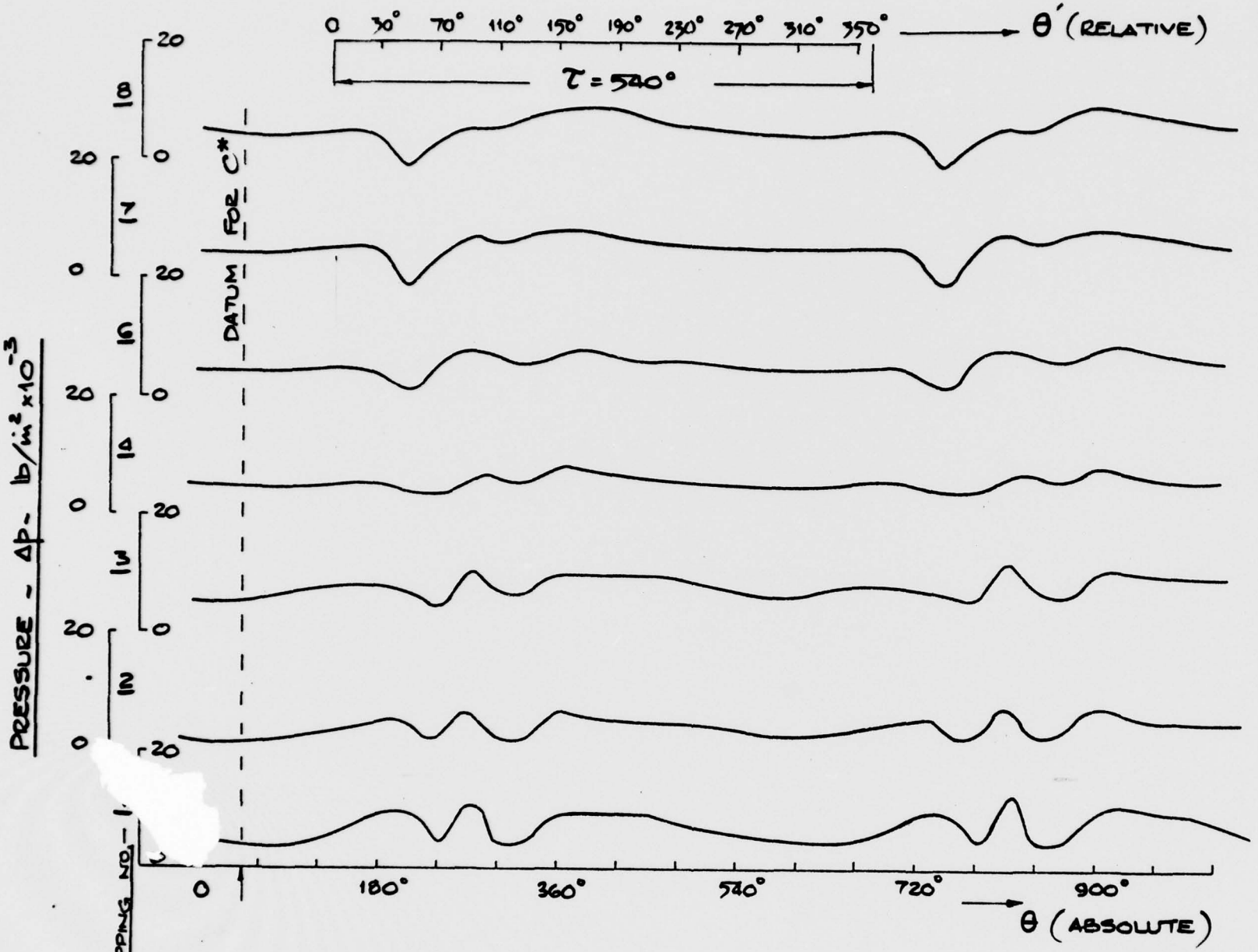

FIG.6. ROTOR PRESSURE SURFACE UNSTEADY PRESSURE MEASUREMENTS

UNDISTURBED INLET FLOW, ROTATING STALL PRESENT

FIG.6

FIG.7

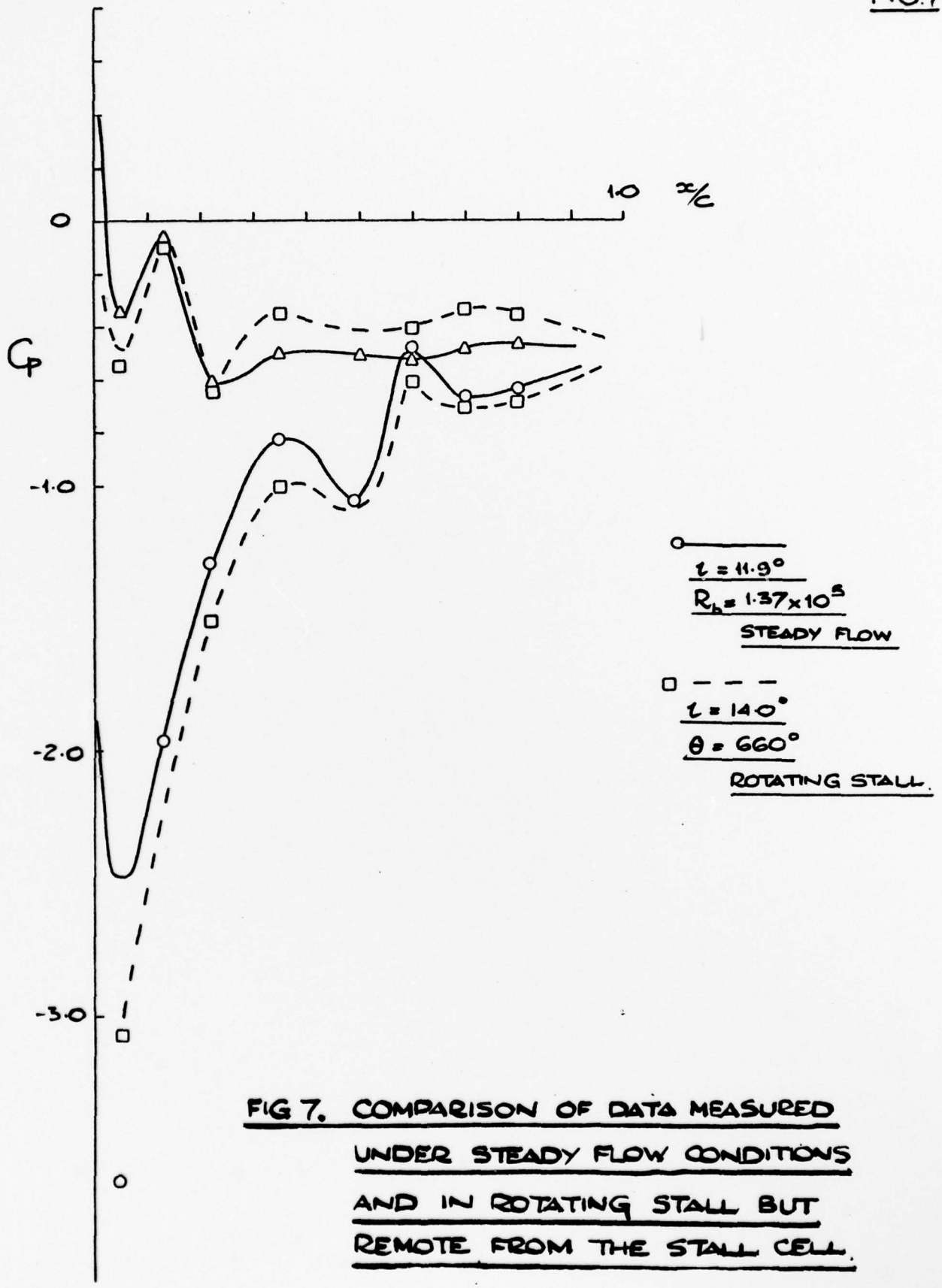

FIG 7. COMPARISON OF DATA MEASURED UNDER STEADY FLOW CONDITIONS AND IN ROTATING STALL BUT REMOTE FROM THE STALL CELL.

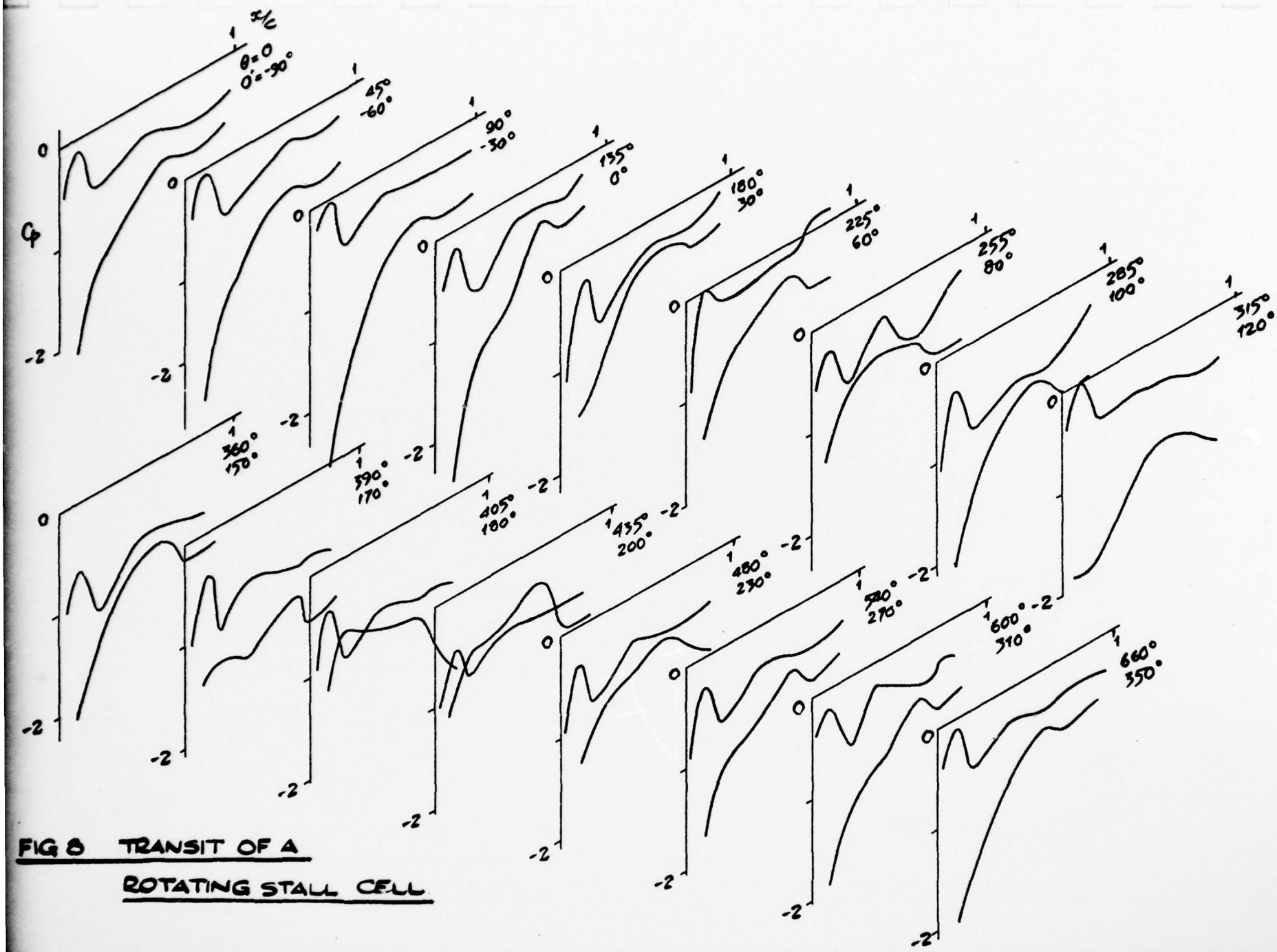

FIG 8 TRANSIT OF A ROTATING STALL CELL

FIG 8

△ PRESSURE SURFACE

○ SUCTION SURFACE

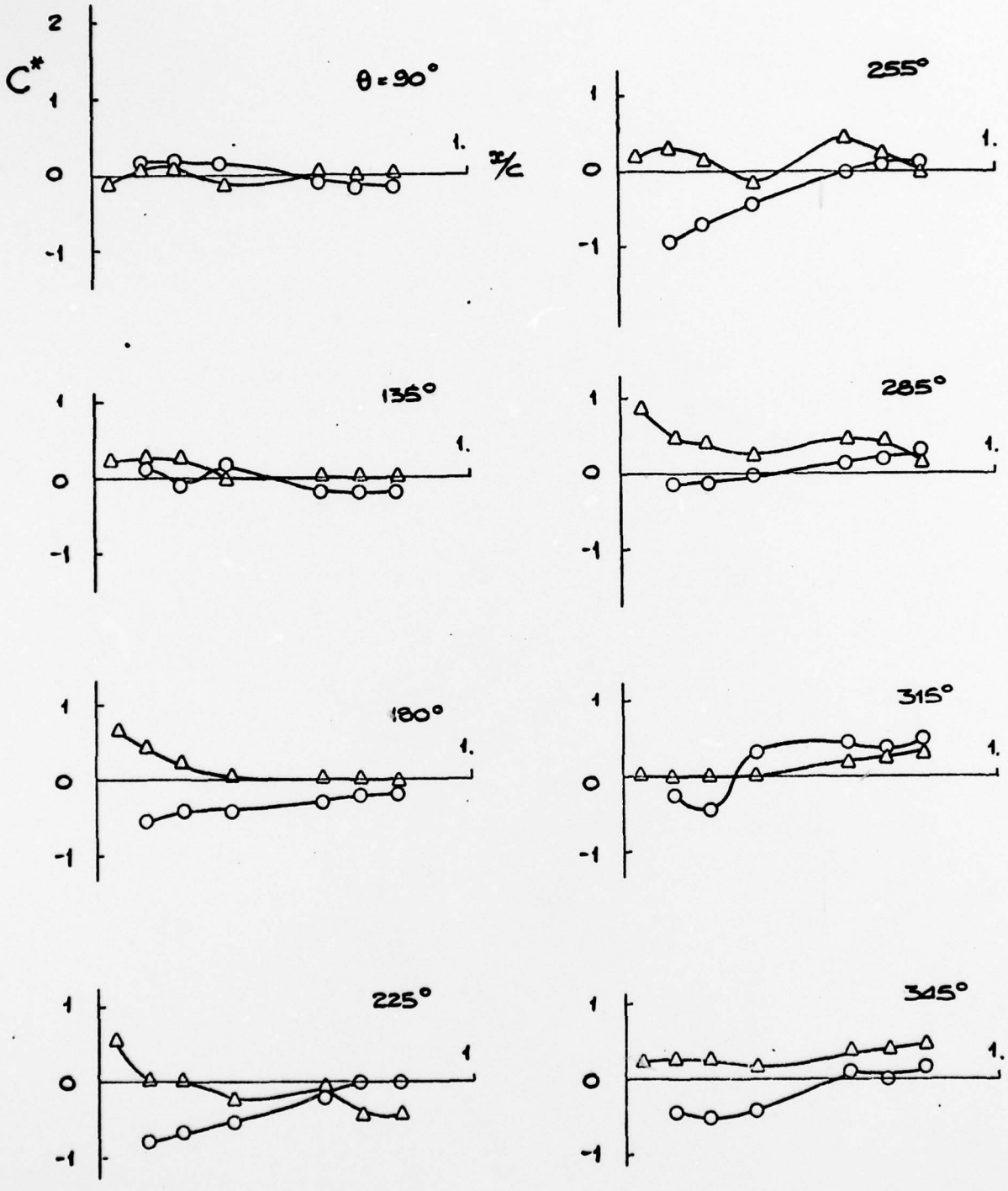

FIG 9. EFFECT OF ROTATING STALL ON THE UNSTEADY PRESSURE COEFFICIENT C^*

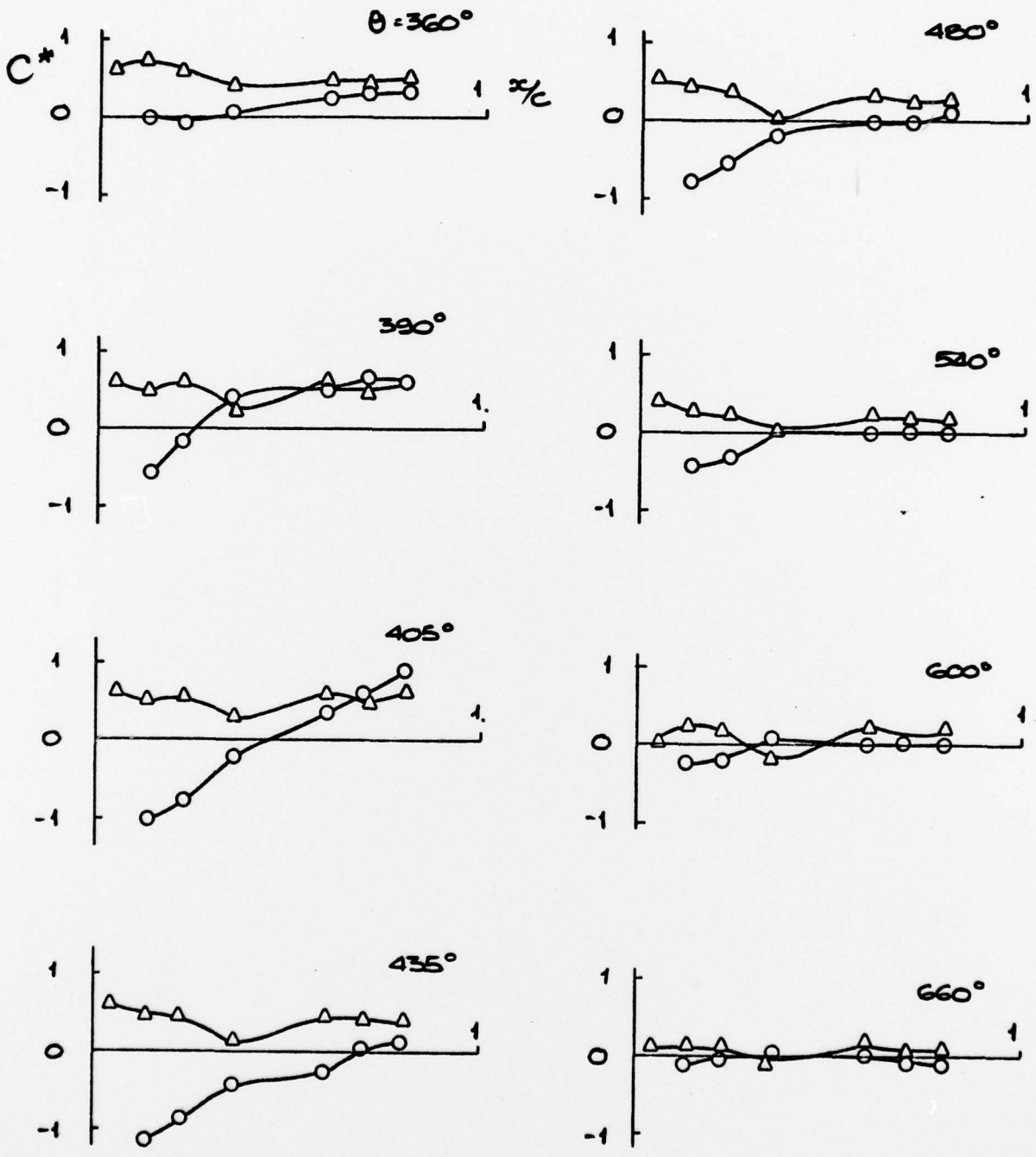
θ=360°
C*
1
0
-1
x/c
480°
390°
540°
405°
600°
435°
660°

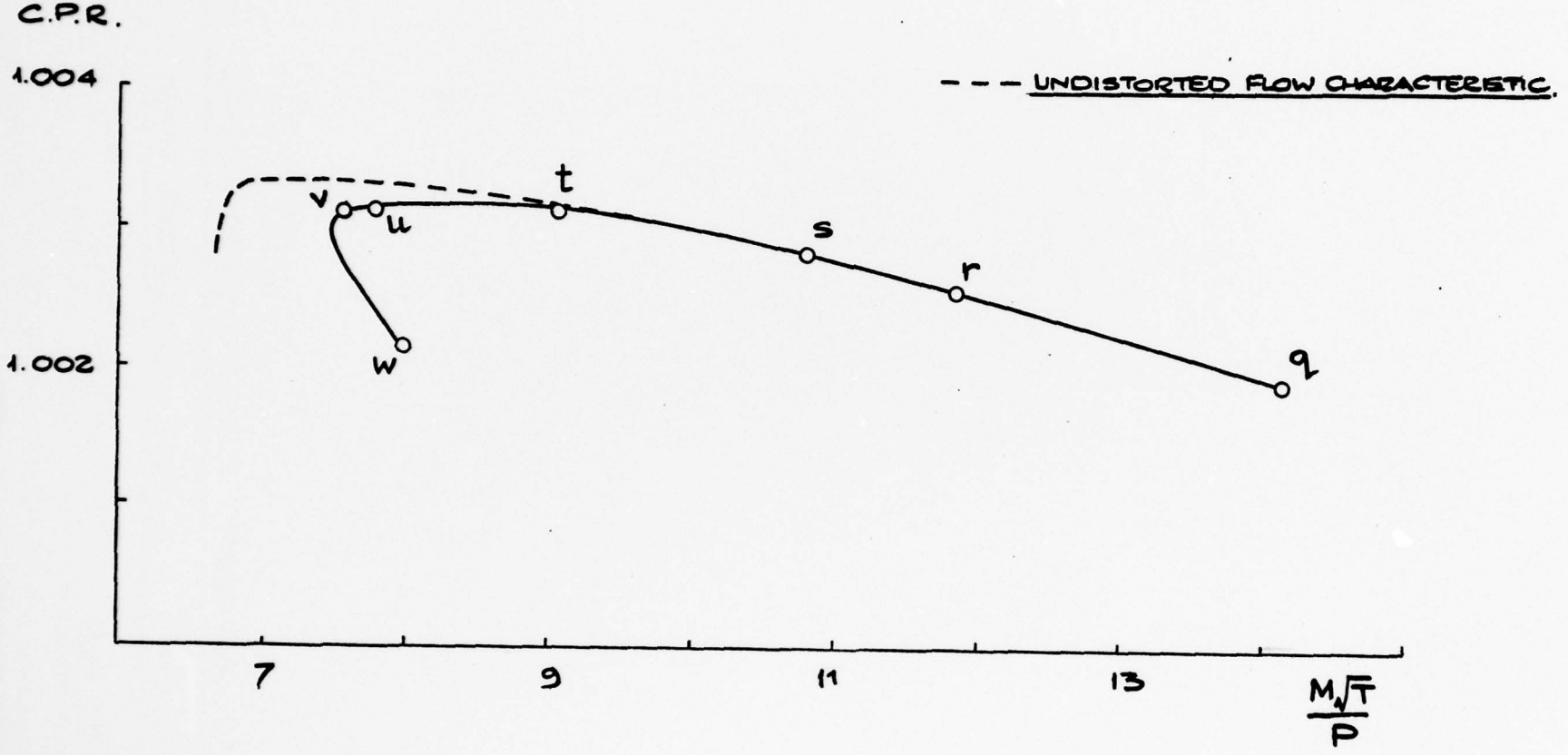

FIG. 10. DISTORTED FLOW COMPRESSOR CHARACTERISTIC - 1250 rev/min : $\theta_D = 90°$

FIG.10

FIG.11

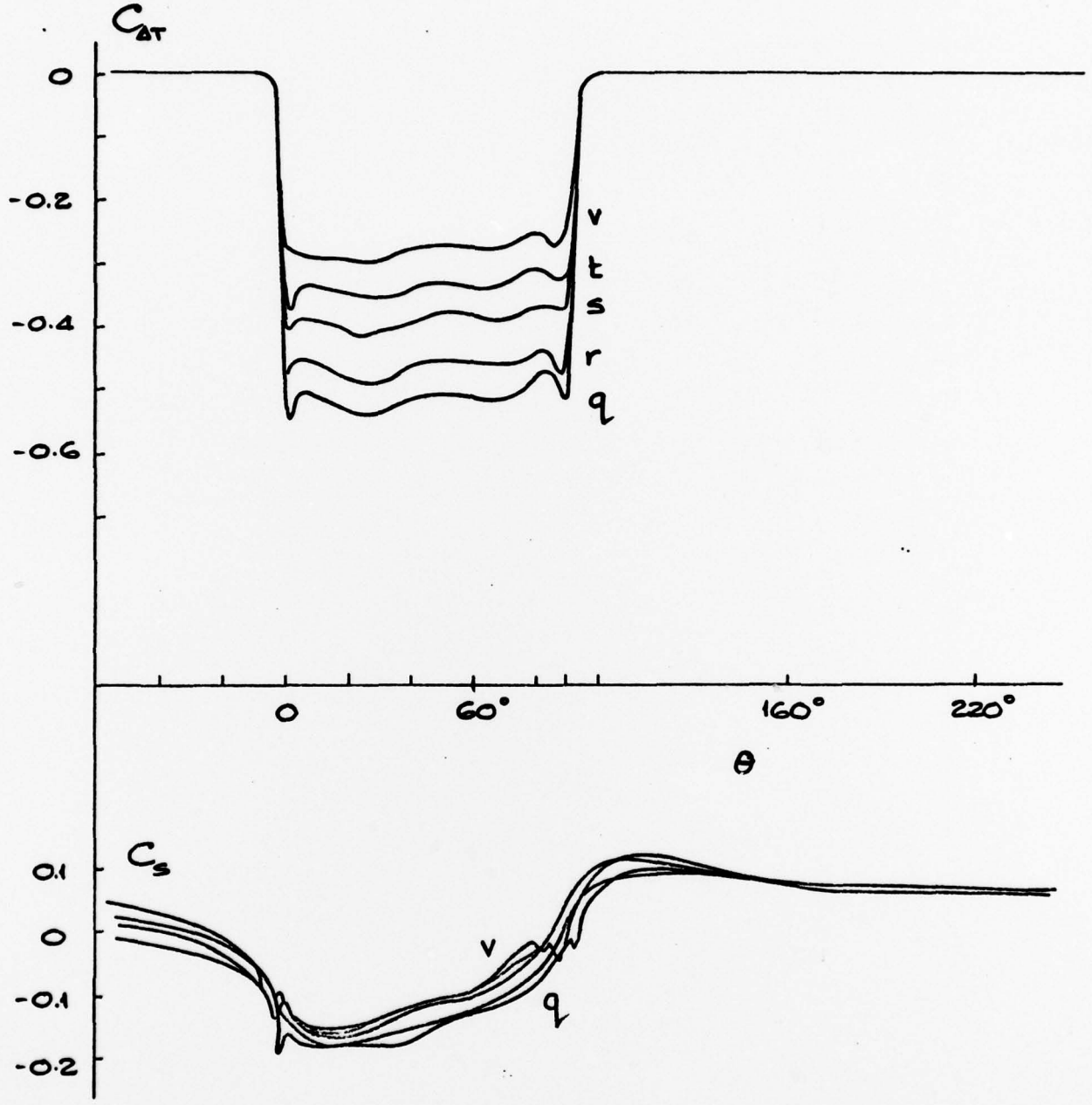

FIG. 11. EFFECT OF COMPRESSOR OPERATING POINT UPON DISTORTION PROFILE - 1250 RPM/min

$\theta_D = 90°$

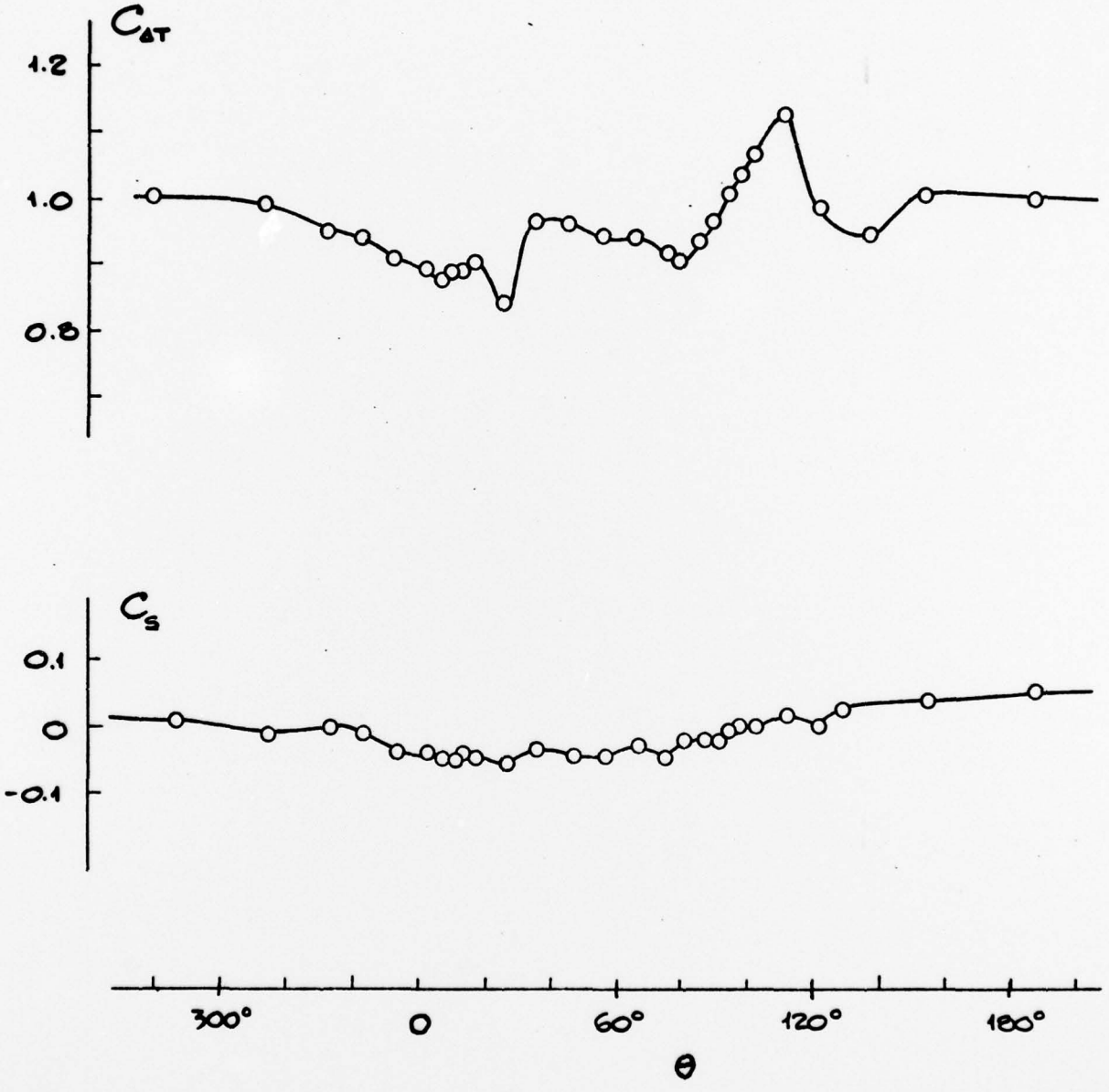

FIG 12. CIRCUMFERENTIAL PRESSURE VARIATION DOWNSTREAM OF COMPRESSOR - 1250 rev/min, POINT 'V', θ_D=90°.

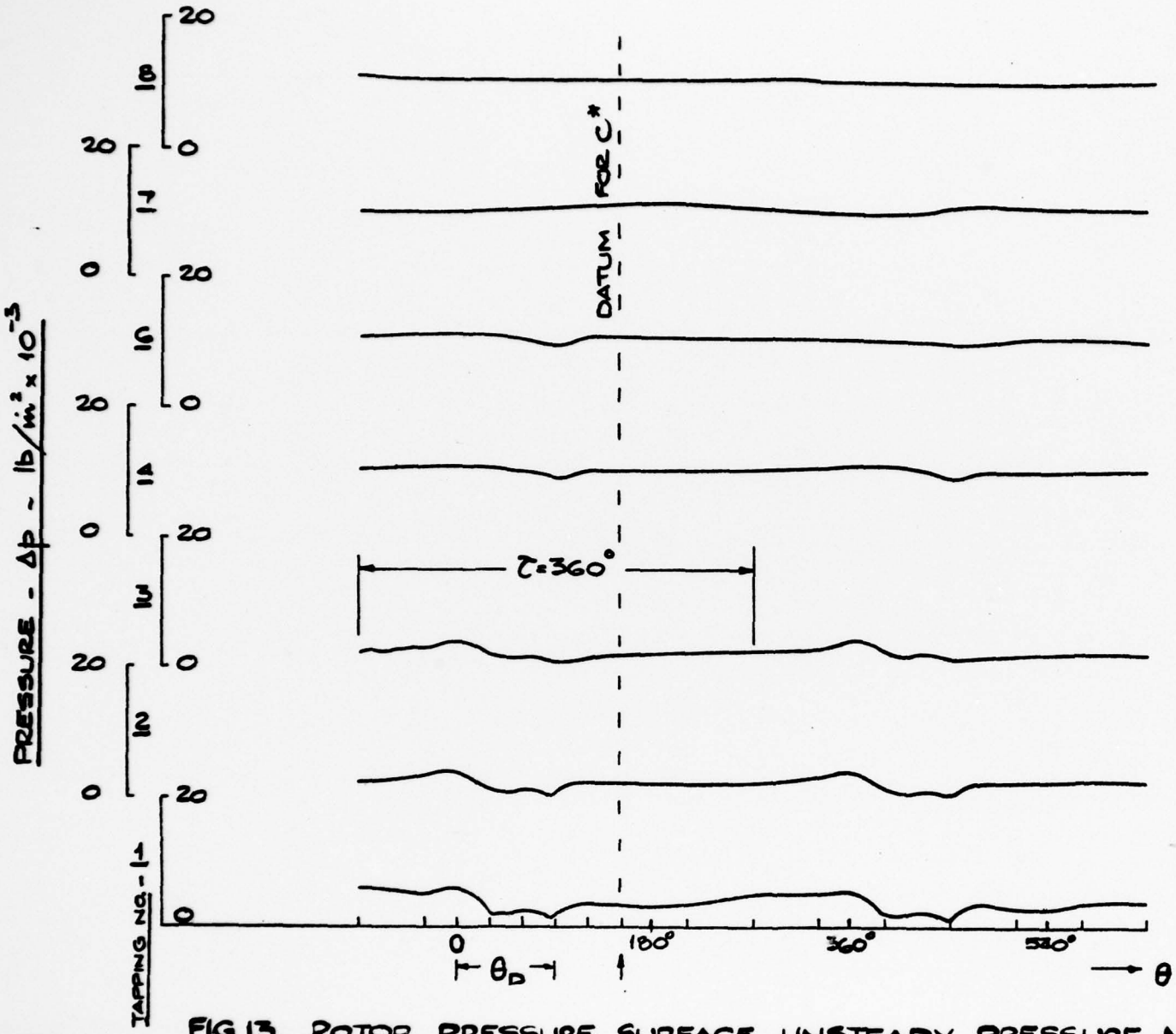

FIG 13. ROTOR PRESSURE SURFACE UNSTEADY PRESSURE MEASUREMENTS

$\theta_D = 90°$, UNSTALLED FLOW

FIG.13.

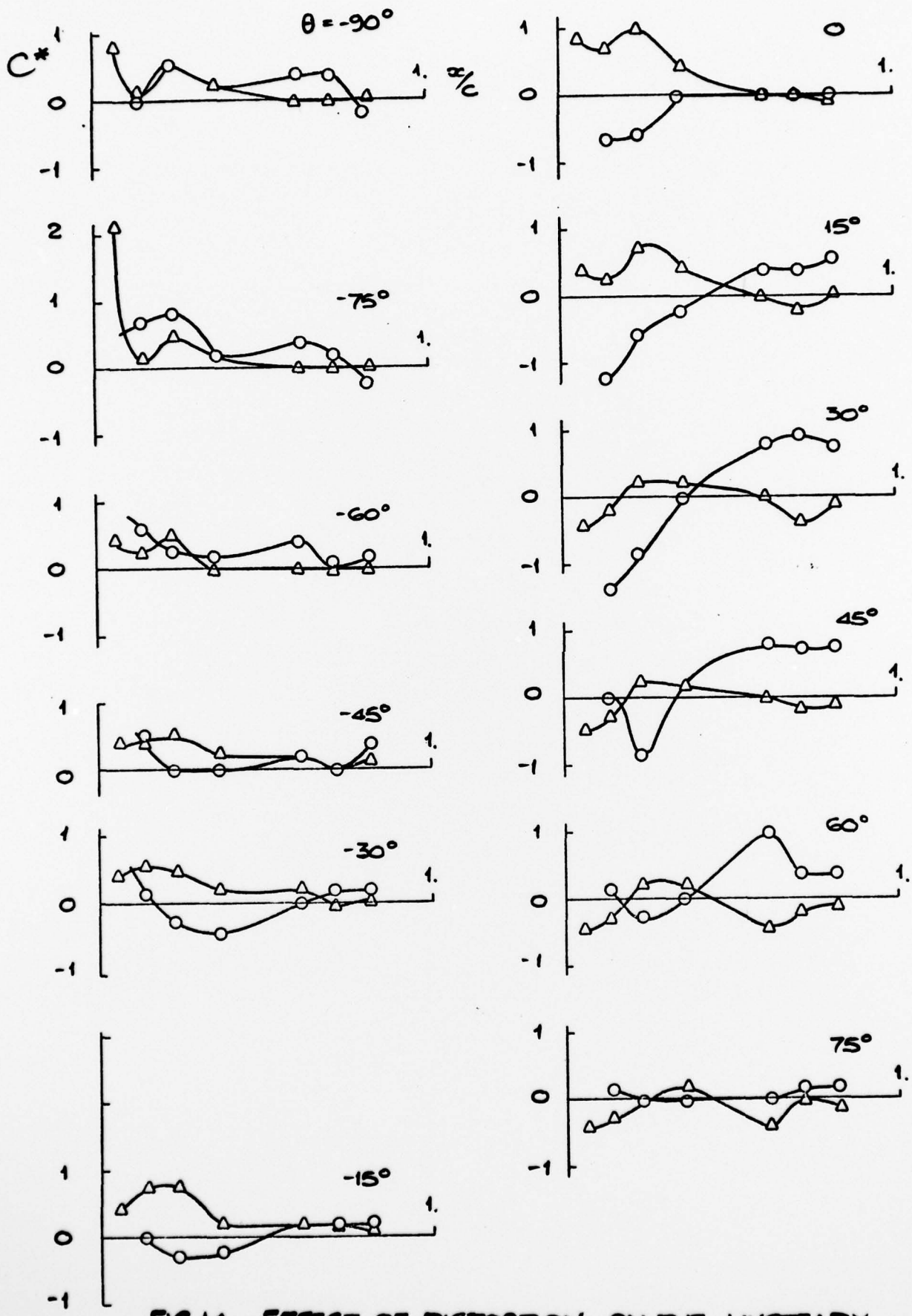

FIG.14. EFFECT OF DISTORTION ON THE UNSTEADY PRESSURE COEFFICIENT C^*

FIG.14 (CONT)

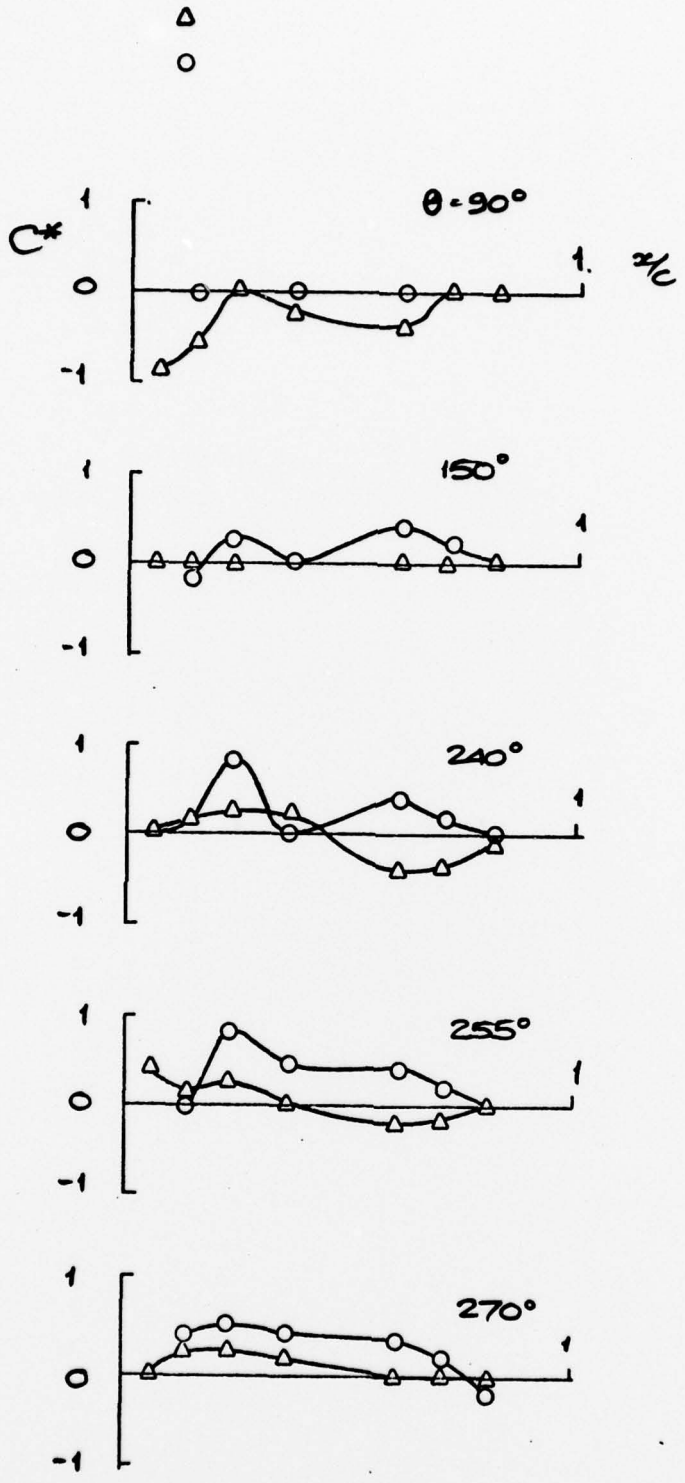

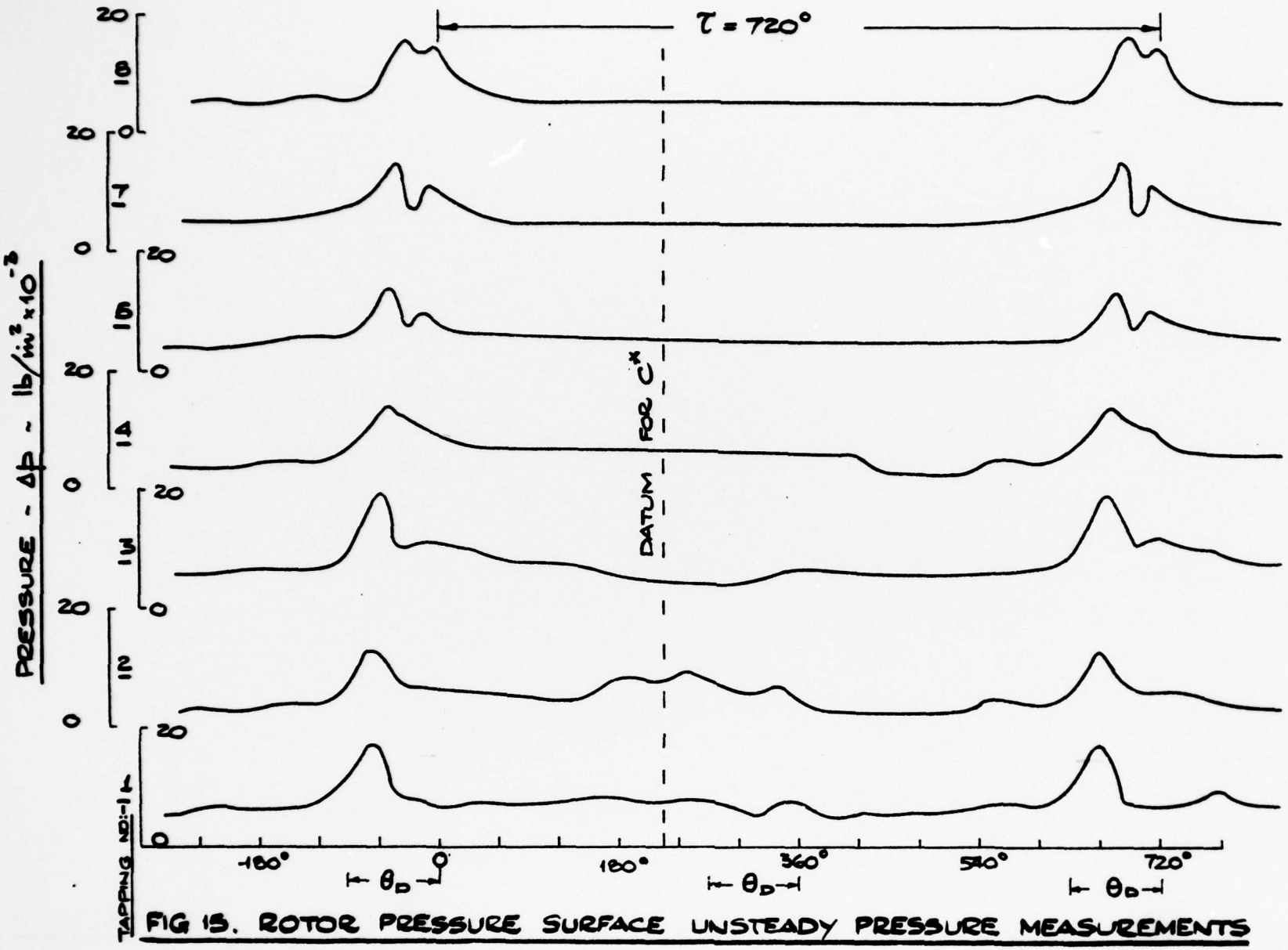

FIG 15. ROTOR PRESSURE SURFACE UNSTEADY PRESSURE MEASUREMENTS

$\theta_D = 90°$, WITH ROTATING STALL.

FIG.15

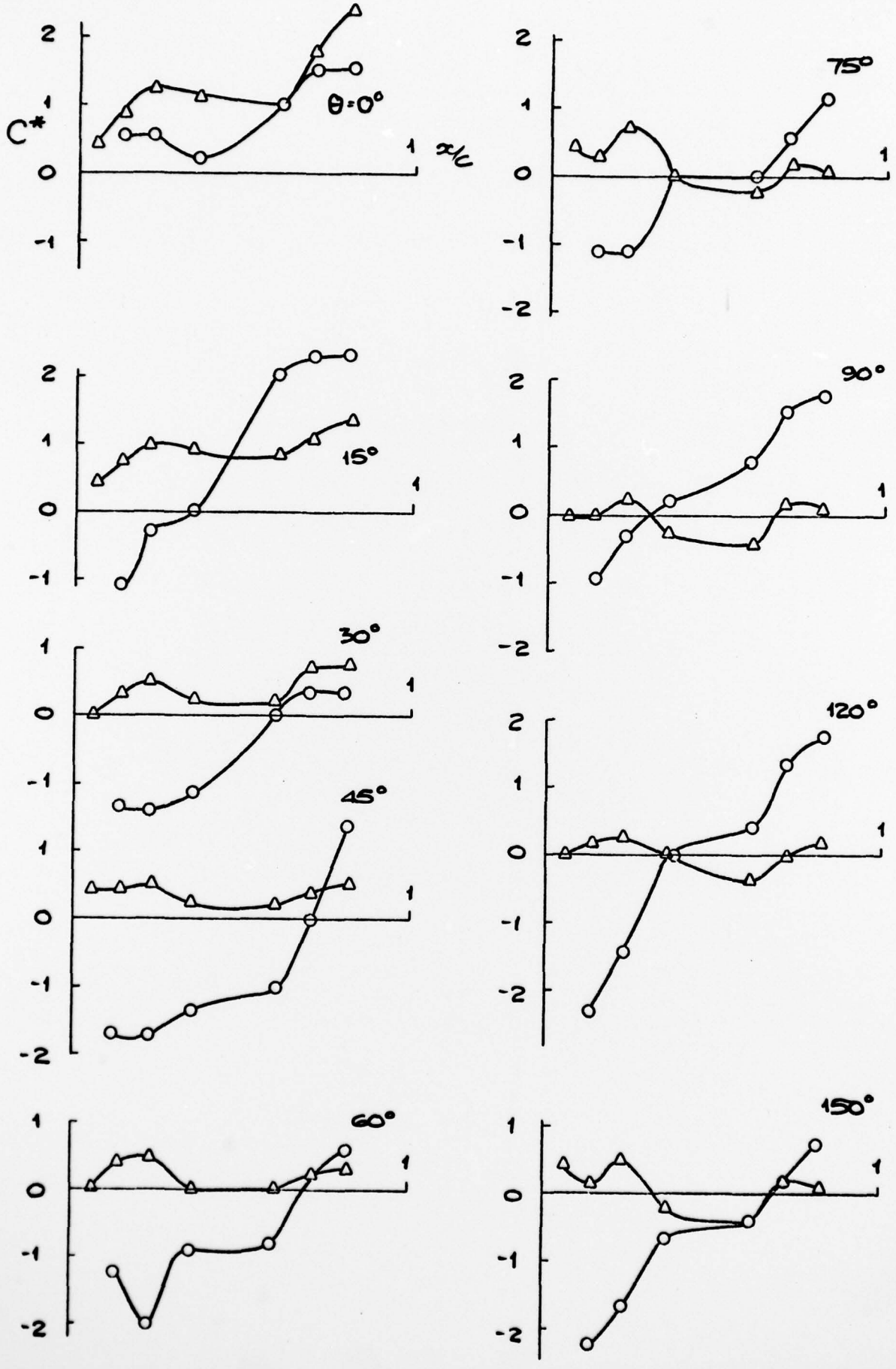

FIG.16. EFFECT OF DISTORTION & ROTATING STALL UPON

FIG.16.(CONT)

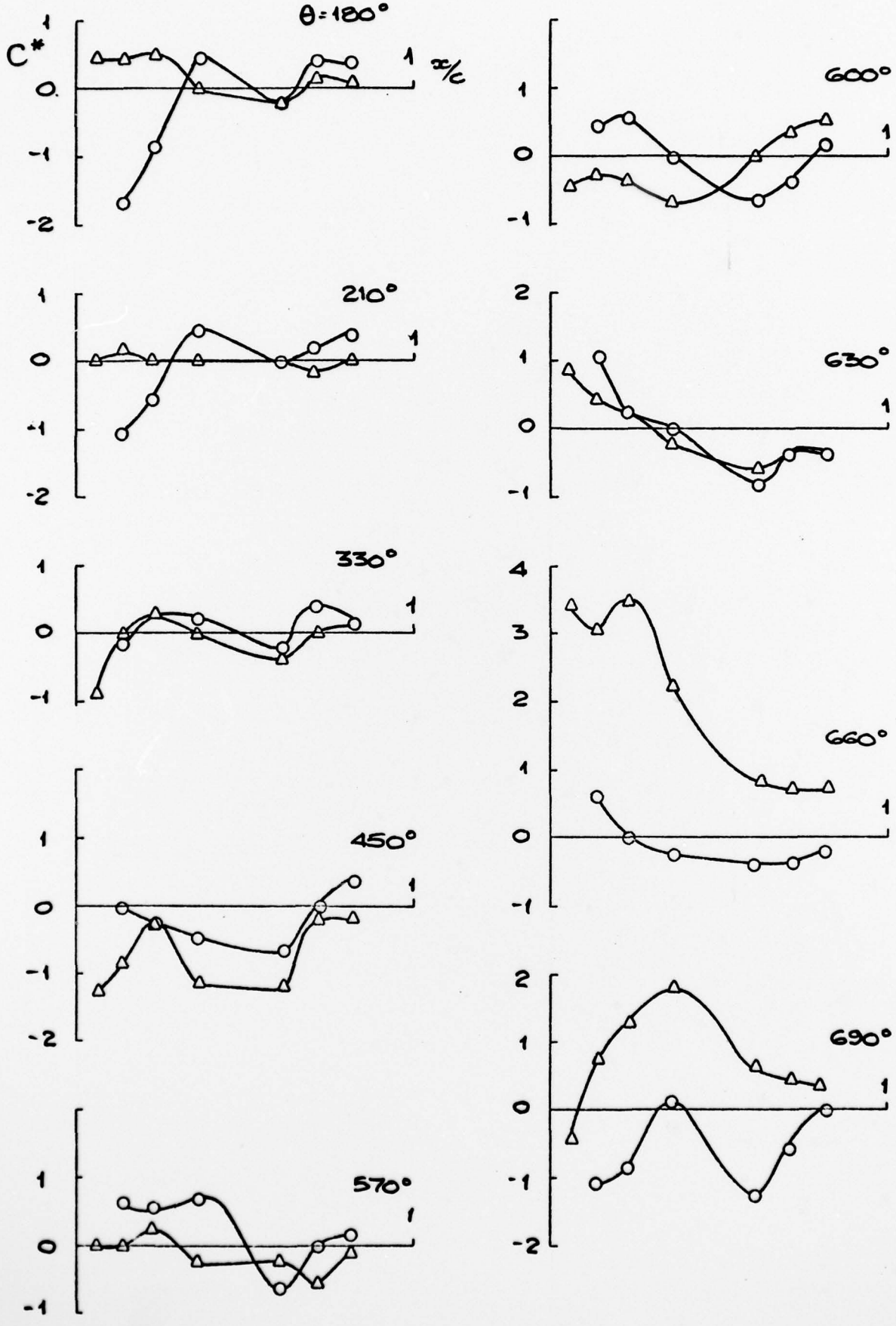

FIG.16(CONT)

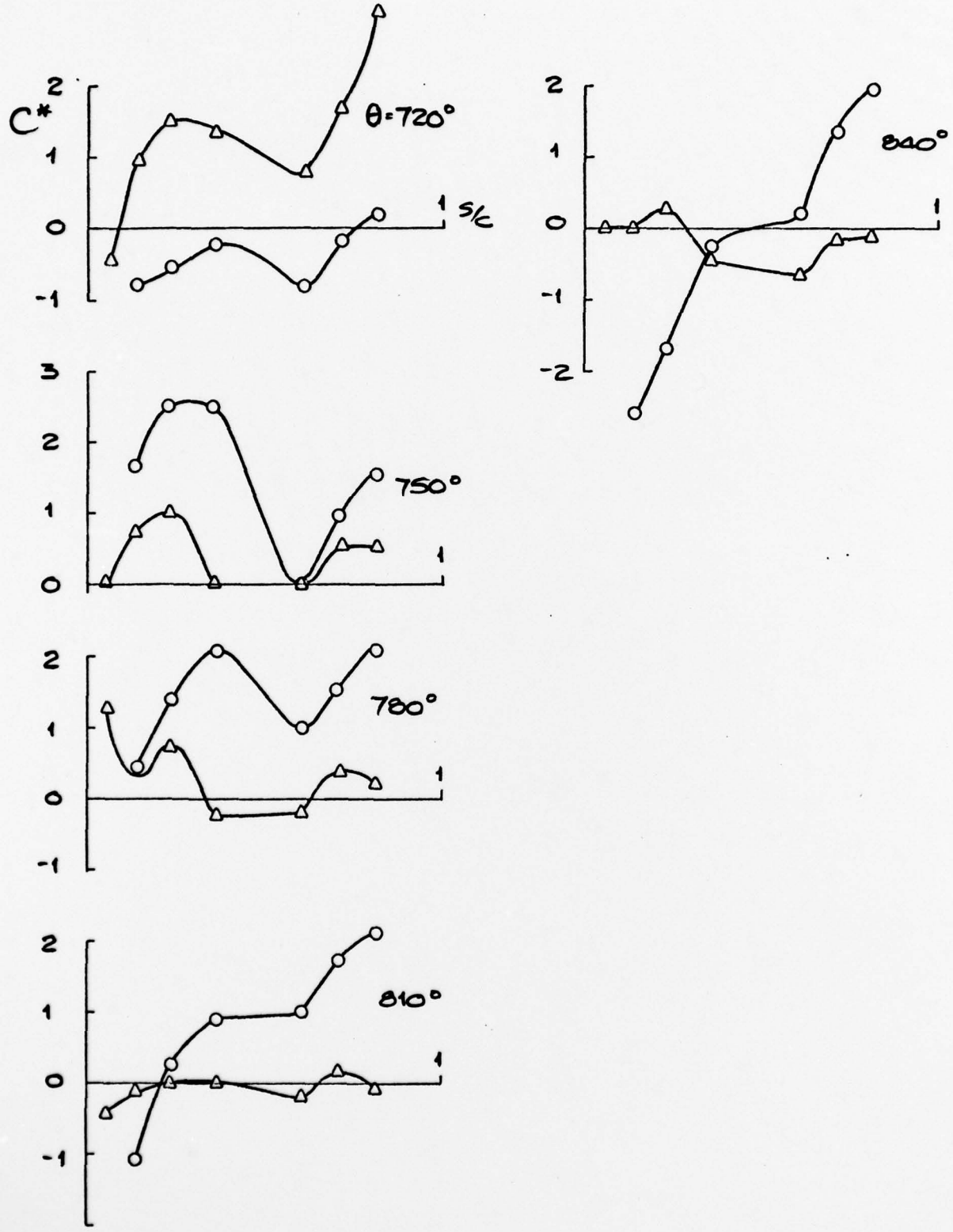

SECURITY CLASSIFICATION OF THIS PAGE *(When Data Entered)*

REPORT DOCUMENTATION PAGE

READ INSTRUCTIONS BEFORE COMPLETING FORM

1. REPORT NUMBER AFOSR-TR- 78-1629	2. GOVT ACCESSION NO. / 3. RECIPIENT'S CATALOG NUMBER
4. TITLE *(and Subtitle)* UNSTEADY EFFECTS OF CIRCUMFERENTIAL PRESSURE DISTORTED INLET FLOWS IN COMPRESSORS	5. TYPE OF REPORT & PERIOD COVERED INTERIM 15 Apr 78 - 14 Oct 78 6. PERFORMING ORG. REPORT NUMBER
7. AUTHOR(s) R E PEACOCK	8. CONTRACT OR GRANT NUMBER(s) AFOSR 77-3305
9. PERFORMING ORGANIZATION NAME AND ADDRESS CRANFIELD INSTITUTE OF TECHNOLOGY SCHOOL OF MECHANICAL ENGINEERING CRANFIELD BEDFORD MK43 OAL ENGLAND	10. PROGRAM ELEMENT, PROJECT, TASK AREA & WORK UNIT NUMBERS 23074A 61102F
11. CONTROLLING OFFICE NAME AND ADDRESS AIR FORCE OFFICE OF SCIENTIFIC RESEARCH/NA BLDG 410 BOLLING AIR FORCE BASE, D C 20332	12. REPORT DATE Nov 78 13. NUMBER OF PAGES 38
14. MONITORING AGENCY NAME & ADDRESS*(if different from Controlling Office)*	15. SECURITY CLASS. *(of this report)* UNCLASSIFIED 15a. DECLASSIFICATION/DOWNGRADING SCHEDULE

16. DISTRIBUTION STATEMENT *(of this Report)*

Approved for public release; distribution unlimited.

17. DISTRIBUTION STATEMENT *(of the abstract entered in Block 20, if different from Report)*

18. SUPPLEMENTARY NOTES

19. KEY WORDS *(Continue on reverse side if necessary and identify by block number)*

TURBOMACHINERY
COMPRESSORS
UNSTEADY AERODYNAMICS INLET MALDISTRIBUTION EFFECTS

20. ABSTRACT *(Continue on reverse side if necessary and identify by block number)*

Using custom designed and developed rotor borne instrumentation rotating stall phenomena are examined in a lightly loaded single-stage compressor. Two different classes of rotating stall are identified and of different rotational frequency. One propagates from the blade loading edge and the other from the blade trailing edge.

DD FORM 1 JAN 73 1473

UNCLASSIFIED
SECURITY CLASSIFICATION OF THIS PAGE *(When Data Entered)*